

MARKUP

COPY

FINAL

**“CATALASAN NUCLEAR FUSION REACTOR”**  
**A High Speed Rotating Centrifugal-Laser**  
**Nuclear Fusion Reactor**

**Mr. Peter Paul Catalasan**

Chief Theoretical Research Scientist:

A Mathematical Physicist,

Theoretical Computer Scientist, and

Artificial Intelligence Researcher

Advanced Catalasan Research Laboratories, Inc.

Citizen of the Republic of the Philippines

Citizen of the United States of America

*CSULB Graduate Student*

United States Residence

25410 Dodge Ave. # K

Harbor City, CA 90710

pcatalasan@yahoo.com

310.830.1046

***Abstract*** – Generations of *Physicists* have attempted to build Thermonuclear Fusion Reactors in hope of harnessing the Energies of the ubiquitous Hydrogen and Hydrogen Nuclear Fusion Reactions similar to our Sun's. With respect to physicists, the failure, I believe, involves overcomplicated design structures. Thus, I have chosen my design as a very practical High-Speed Rotating Centrifugal-Laser Nuclear Fusion Reactor, a design based on Demirkhanov's Solenoid Experiment where plasma is trapped radially by an intense electromagnetic field induced by a powerful Solenoid. In my idea, the Solenoid's plasma is then heated on one end of the solenoid cylinder with a Free-Electron Laser, which is also a working Laser Fusion Device. [used by *Nuclear Fusion Physicists*.] And, on the other end of the solenoid cylinder, a Centrifugal Force is applied linearly to the plasma by revolving the entire Solenoid at its end on its primary axis. Since Demirkhanov's system works and also its Free-Electron Laser, it follows that this Nuclear Fusion Reactor will also work, having Demirkhanov's working system a viable proof of experimentation.

# “CATALASAN NUCLEAR FUSION REACTOR”

## A High Speed Rotating Centrifugal-Laser

### Nuclear fusion reactor

#### **Mr. Peter Paul Catalasan**

Chief Theoretical Research Scientist:

A Mathematical Physicist,

Theoretical Computer Scientist, and

Artificial Intelligence Researcher

Advanced Catalasan Research Laboratories, Inc.

Citizen of the Republic of the Philippines

Citizen of the United States of America

*CSULB Graduate Student*

United States Residence

25410 Dodge Ave. # K

Harbor City, CA 90710

pcatalasan@yahoo.com

310.830.1046

#### Table of Contents

- I. Field of Invention
- II. Summary of Invention
- III. System Drawings
- IV. Brief Description of Drawings
- V. Description of the Preferred Embodiments
- VI. Theoretical Calculations
- VII. [Reference] Bibliography

#### I. Field of Invention

The established knowledge necessary to understand encompass Mechanics, Advanced Mechanics of Materials, Thermodynamics, Electromagnetic Fields, Plasma, and Laser Physics; having the field of invention in Nuclear Fusion Research.

#### II. Summary of Invention

The fundamental idea of my invention is to use a large high-speed centrifugal rotating Disk with many lasers attached at the ends of the disk in order to confine plasma, where the force of the laser and the force of the centrifuge are in opposite equilibrium. And linearly, to guide the Plasma, that is proton-injected by an electronic toggle switch of positive and negative charge at the equilibrium position, into a radial cross section, we use Demirkhanov's high-intense electromagnetic field solenoid confinement, with powerful electromagnetic fields at the ends in order to pinch the plasma. Whenever the Plasma is exhausted of useful energy, a highly tunable laser attached at the ends of the disk, increases its force in order to push the Plasma into the center hole of the rotating disk, through releasing the plasma by lowering the powerful electromagnetic fields toward the center at the solenoid's end, where it is pushed down by an

electromagnetic field from a small circular current-carrying magnet into a plasma exhaust system. The plasma exhaust system is also a solenoid and with another highly tunable laser, it pushes the used plasma out of the nuclear fusion reactor. [Please see the following Drawings.]

### III. System Drawings

Please see drawing pages.

### IV. Brief Description of Drawings

My choice of explaining my drawings to start from the very simple and to build to the more complex, will help the reader understand this system's workable nature in a step by step process from the experimental beginning to the final design of the Catalasan Rotating Centrifugal-Laser Nuclear Fusion Reactor. [Let's begin a brief introduction with drawings.]

Demirkhanov's Solenoid Experiment: A Working System, *Drawing 1*, consists of a Solenoid: an Electromagnetic Porous Cylinder Material, **Fig. 1**; Copper Coils, **Fig. 2**, wrapped around the Electromagnetic Porous Cylinder Material, **Fig. 1**; Negative Voltage  $-V$ , **Fig. 3**, and Positive Voltage  $+V$ , **Fig. 4**, in order to cause a current through the Copper Coils, **Fig. 2**; with Plasma confined radially in a Vacuum, **Fig. 5**. [Please note that] This system already works due to Demirkhanov's Experimentation with Solenoids and Plasma.

Free-Electron Lasers: A Working Device, *Drawing 2*, use Magnets, **Fig. 6**, and Free Electrons, **Fig. 9**, to cause electrons to bounce back and forth between the Total Reflector, **Fig. 7**, and Output Mirror, **Fig. 8**, creating Light Amplification through Stimulated Emission of Radiation, or LASER. Respectively, this device works as well.

Peter Paul Catalasan's Solenoid-Laser System: A Copy of Demirkhanov's Solenoid Experiment with an Addition of Free-Electron Lasers and a Proton Injection Device, *Drawing 3*, uses a Proton Injection Device, **Fig. 10**, located midway between the Solenoid in order to input pre-plasma protons. Given Demirkhanov's Solenoid, an addition of two Free-Electron Lasers, **Fig. 11 & Fig. 12**, on the outer ends of the Solenoid, causes plasma confinement radially and in the center of the Solenoid. [As explained earlier,] This Solenoid consists of an Electromagnetic Porous Cylinder Material, **Fig. 15**; Copper Coils, **Fig. 13**, wrapped around the Electromagnetic Porous Cylinder Material, **Fig. 15**; Negative Voltage  $-V$ , **Fig. 17**, and Positive Voltage  $+V$ , **Fig. 16**, in order to cause a current through the Copper Coils, **Fig. 13**; Electromagnetic Plasma Pinchers, **Fig. A & Fig. D**, with Variable Pincher Voltage,  $-V_{pv}$  &  $+V_{pv}$ , **Fig. B & Fig. C**, and fixed Pincher Voltage,  $-V_{ps}$  &  $+V_{ps}$ , **Fig. E & Fig. F**; with Plasma confined radially in a Vacuum, **Fig. 14**. Thus the only additions are the two Free-Electron Lasers, **Fig. 11 & Fig. 12**, Proton Injection Device, **Fig. 10**, and two high-intense Electromagnetic Plasma Pinchers, **Fig. A & D**, in order to completely confine the Plasma. Since Free-Electron Lasers work, the Proton Injection Device very simple,

and Electromagnetic Plasma Pinchers basic, this should work as well.

Peter Paul Catalasan's Centrifugal-Laser System: A Copy of Demirkhanov's Solenoid Experiment with an Addition of a Free-Electron Laser and a Proton Injection Device in a Centrifuge, *Drawing 4*, uses a Centrifugal Force, **Fig. 18**, equivalent to the Laser Force, **Fig. 19**, of one Free-Electron Laser replacing the laser at the other end by revolving the entire Solenoid at its end on its primary axis. This causes equilibrium between the Force of One Free-Electron Laser, **Fig. 24**, and Centrifugal Force, **Fig. 18**, at the point of the Proton Injection Device, **Fig. 20**. And, the Electromagnetic Plasma Pincher, **Fig. A & Fig. D**, seals the Plasma at its ends. Thus, [again,] Plasma, **Fig. 21**, is confined radially and at its center by the equilibrium forces, in a Vacuum, **Fig. 22**. Again, there is an Electromagnetic Porous Cylinder Material, **Fig. 23**, and a Positive Voltage  $+V_s$ , **Fig. 25**, Negative Voltage  $-V_s$ , **Fig. 26**, of the Copper Coils. The One Free-Electron Laser, **Fig. 24**, [have] has Positive Voltage  $+V_L$ , **Fig. 27**, Negative Voltage  $-V_L$ , **Fig. 28**, in order to create Light Amplification through Stimulated Emission of Radiation, or LASER. Since Demirkhanov's Solenoid and One Free-Electron Laser [works] work, the only difference is the Centrifugal Force that replaces on one of its end, a Free-Electron Laser, and the two Electromagnetic Plasma Pinchers. [Respectively,] Up to this point, there exists experimental evidence this system will work.

Rotating Centrifugal-Laser Disk System: A High-Speed Rotating Centrifuged, Proton Injected, and Free-Electron Laser Heated, Disk System, *Drawing 5*, rotates counterclockwise with Free-Electron Lasers attached at the ends, **Fig. 29**, with Peter Paul Catalasan's Centrifugal-Laser System, **Fig. 30**, and the Proton Injection Device in the equilibrium position, **Fig. 31**. Peter Paul Catalasan's Centrifugal-Laser System is tilted in order that the Free-Electron Lasers attached at the ends do not shoot each other, **Fig. 32**. The tilt at the center hole, **Fig. 33**, shows Free-Electron Laser paths that push the Plasma, when it is no longer useful for energy, lowering one side of the Solenoid at the end toward the center the Variable Electromagnetic Plasma Pincher, **Fig. M**, into the center hole and into the Plasma Exhaust System. The Energy released is absorbed by the Electromagnetic Porous Cylinder Material transferring heat energy to the Heat Sink, **Fig. 34**, and into the surrounding water medium.

Peter Paul Catalasan's Centrifugal-Laser System: A Copy of Demirkhanov's Solenoid Experiment with an Addition of a Free-Electron Laser and a Proton Injection Device in a Centrifuge, *Drawing 6*, consist of a Proton Injection Device, Electrical Wire System, Demirkhanov's Solenoid Experiment, and a Free-Electron Laser, Electromagnetic Plasma Pinchers, and Plasma Exhaust System. The Proton Injection Device consist of the Proton Pump from the outside, **Fig. 34**, Proton Capture, **Fig. 35**, and Proton Rotating Mechanical Seal, **Fig. 36**, where the Proton is pushed down into the Proton Injection Device, that contains a small Electrical Switch, **Fig. 40**, toggling between positive and negative charge in order to trap them and push two protons into Demirkhanov's Solenoid. The Electrical Wire System consists of Wire Inputs, **Fig. 37**, Rotating Wire Contacts, **Fig. 38**, Electrical Wires, **Fig. 39**, and a Wire Rotating Mechanical Seal. The Electrical Wires contain wires from the Free-Electron Laser,  $+V_L$  &  $-V_L$ , Demirkhanov's Solenoid,  $+V_s$  &  $-V_s$ , Variable Electromagnetic Plasma Pincher,  $-V_{pv}$  &  $+V_{pv}$ , Fixed Electromagnetic Plasma Pincher,  $-V_{ps}$  &  $+V_{ps}$ , Plasma Exhaust

Solenoid,  $+V_E$  &  $-V_E$ , and Electromagnetic Plate, **Fig. 41**,  $+V_P$  &  $-V_P$ . The Plasma Exhaust System consists of an Electromagnetic Plate, **Fig. 41** & **Fig. 42**, an Exhaust Solenoid, **Fig. 44**, with Copper Coils, **Fig. 43**. Finally, the Proton Injection Device, Demirkhanov's Solenoid and Free-Electron Laser, Electrical Wire System, two Electromagnetic Plasma Pinchers, and Plasma Exhaust System are all enclosed by Titanium, **Fig. 45**. The Plasma Exhaust System: Exploded View, *Drawing 7*, consist of the Titanium Steel, **Fig. 46**, Rotating Mechanical Seal, **Fig. 47** & **Fig. 48**, Exhaust Solenoids, two Free-Electron Lasers from the outside, Plasma Exit Solenoids, and Electrical Wire System, **Fig. 49**, containing Exhaust Solenoid Voltages,  $-V_E$  &  $+V_E$ , all rotating counterclockwise.

The last drawing, the Catalasan Centrifugal-Laser Nuclear Fusion Reactor: A High-Speed Rotating Centrifugal-Laser & Steam-Turbine Nuclear Fusion Reactor, designated as the Main Drawing, *Drawing 8*, is the integration of a Flip-Flopped Rotating Centrifugal-Laser Disks System, **Fig. 58**, Plasma Exhaust System, **Fig. 57**, Steam Turbine System, **Fig. 50**, and Electric Turbine Generator, **Fig. 61**. The Flip-Flopped Rotating Centrifugal-Laser Disk System, **Fig. 58**, consists of the Rotating Centrifugal-Laser Disk System, *Drawing 5*, stacked such that the Plasma Exhaust System is joined together and the Proton Pump, Proton Injection System, and Electrical Wire System on, *Drawing 6*, are also joined together, **Fig. 57**, all rotating through the Steam-Turbine Gear System, **Fig. 52**, due to Steam, **Fig. 51**, passing through Steam Turbines, **Fig. 50**. The Steam, then, is condensed through a Steam Condenser, **Fig. 54**, through Steam Pipes, **Fig. 53**, and into the  $H_2O$  Reservoir, **Fig. 55**, which is then connected by an Open Valve, **Fig. 56**, back into the Reactor. The Rotation caused by the Steam-Turbine Gear, **Fig. 52**, is then translated, by the Axel, **Fig. 60**, to the Electric Power Turbine Generator, **Fig. 61**, generating commercial electricity, **Fig. 62**, with an initial Gas Powered Engine Starter, **Fig. 59**.

## V. Description of the Preferred Embodiments

Scientists, including myself, have dreamed of building thermonuclear fusion reactors in hope of harnessing high-energy nuclear reactions similar to our Sun's for a clean and radioactive-free energy supply. The energy reactions associated with these machines require initial proton and proton nuclear reactions as follows:  $p + p \rightarrow {}^2H + e^+ + \nu$ , with energy yield 0.42 MeV;  $e^+ + e^- \rightarrow \gamma$ , with energy yield 1.02 MeV;  ${}^2H + p \rightarrow {}^3He + \gamma$ , with energy yield 5.49 MeV; where the first three previous reactions occur twice and one for  ${}^3He + {}^3He \rightarrow {}^4He + p + p$ , with energy yield 12.86 MeV; producing a combined energy yield of 26.72 MeV for just a few initial number of protons,  $2(2p + p) - 2p = 4p$ . And the number of protons equal to  $4p \cdot N_p$ , where  $4p \cdot N_p = 26.72 \cdot N_p$  MeV and  $N_p$  equals the multiple numbers of  $4p$ . The objective now is then to create any containment device whether electromagnetic, mechanical, or laser, etc. The containment system I have chosen covers many forms that encompass most areas of physics, being electromagnetic, centrifugal, laser, and mechanical.

We begin first with electromagnetism, namely Demirkhanov's Solenoid Experiment, *Drawing 1*, which is already a working device, called the "UMIST Linear System (ULS)". The plasma source in this device

is a duoplasmatron of the type developed by Demirkhanov, which injects a small radius plasma beam into a cylindrical vacuum vessel in the field of a strait solenoid, which confines plasma radially. At the other end of the solenoid is a target area where interactions of the beam can be studied. Recent experiments have used a gas target separated from the rest of the vessel by a septum with a small central hole through which the beam passes. Pressures up to about one Pascal can be maintained in the target area without much effect of the beam at the source end of the vessel [4]. In continuation of his experiment, we increase the solenoid's electromagnetic capacity to pressures beyond one Pascal, into the realms of nuclear fusion. Given the simplicity of a strait solenoid, plasma stability issues outperform any other electromagnetic confinement device. And, in addition, an Electromagnetic Plasma Pincher at the ends of the Solenoid further confines the plasma to keep the plasma from leaking. [If this confinement system does not bear fruit, I believe that we can never attain a nuclear fusion reactor, since nuclear fusion confinement issues usually involve applications of electromagnetic fields, and this is just the basic.]

Secondly, the next confinement system, centrifugal, involves revolving the solenoid at its end and on its primary axis counterclockwise in order to push plasma linearly outward toward the ends of the solenoid whereby a highly tunable laser attached at the end counters its force causing the plasma to remain in equilibrium position, in which the equilibrium centrifugal force is given on, Page 18, the Theoretical Calculation of the Plasma Centrifugal-Laser Equilibrium Force. The number of solenoids attached on a Rotating Centrifugal-Laser Disk System, *Drawing 5*, is  $N_L = (2 \cdot \pi) / (S+L) \cdot (R-L)$ , all revolving counterclockwise, with an angular velocity,  $\omega$ , of the Disk System.

The third confinement, Free-Electron Lasers, *Drawing 2*, slowly heats the Plasma to Nuclear Fusion Temperatures of  $4 \times 10^8$  Kelvin [5] that maintains the Equilibrium Position between the Force of the Laser and the Force of the Centrifuge. Once the Plasma exhausts its energy, the highly tunable Free-Electron Laser, then, pushes the Plasma to the Center Hole of the Disk System, lowering the Variable Electromagnetic Plasma Pincher's strength, whereby an Electromagnetic Plate pushes it into the Plasma Exhaust System. The radiation from a free-electron laser is produced from free electrons, which are forced to oscillate in a regular fashion by an applied field. They are therefore more like synchrotron light sources or microwave tubes than like other lasers. They are able to produce highly coherent, collimated radiation over a wide range of frequencies. The magnetic field arrangement, which produces the alternating field, is commonly called a "wiggler" magnet. The free-electron laser is a highly tunable device, which has been used to generate coherent radiation from  $10^{-5}$  to 1 cm in wavelength. In some parts of this range, they are the highest power source. Particularly in the mm wave range, they exceed all other sources in coherent power. Free-Electron Lasers involve relativistic electron beams propagating in a vacuum and can be tuned continuously, filling in frequency ranges, which are not reachable by other coherent sources. Applications of free-electron lasers are envisioned in isotope separation, plasma heating for nuclear fusion, and particle acceleration in accelerators [4].

The last confinement, material, must overcome high-intense mechanical requirements used for the

*Catalasan Centrifugal-Laser Nuclear Fusion System*, namely Titanium Alloy. Major industrial applications for Titanium remains in heat transfer applications in which the cooling medium is seawater, brackish water, or polluted water, Titanium Condensers, shell and tube heat exchangers, and plate and frame heat exchangers are used extensively in power plants, refineries, air conditioning systems, chemical plants, offshore platforms, surface ships and submarines. The life span and dependability of Titanium are demonstrated by the fact that millions of feet of welded Titanium tubing in power plant condenser service, there have been no reported failures due to corrosion of the cooling water side. And, Titanium alloys are highly resistant to water, natural water and steam to temperatures in excess of 570° F (300° C) [4]. Thus, given the fact that these confinement mechanisms work, it implies that the composition of these devices into one unified system, will also work explained by the following text.

Demirkhanov's Solenoid Experiment: A Working System, *Drawing 1*, consists of a Solenoid: an Electromagnetic Porous Cylinder Material, **Fig. 1**; Copper Coils, **Fig. 2**, wrapped around the Electromagnetic Porous Cylinder Material, **Fig. 1**; Negative Voltage  $-V$ , **Fig. 3**, and Positive Voltage  $+V$ , **Fig. 4**, in order to cause a current through the Copper Coils, **Fig. 2**; with Plasma confined radially in a Vacuum, **Fig. 5**. [Please] Note that this system already works due to Demirkhanov's Experimentation with Solenoids and Plasma. The continuation of Demirkhanov's Solenoid follows. The Electromagnetic Porous Cylinder Material, **Fig. 1**, although unknown to me of the material Demirkhanov used, was able to contain Plasma radially, and in effect had the ability to experiment with linear ion beam targets to study the behavior of the Plasma within the electromagnetic field induced by the Solenoid. The Copper Coils, **Fig. 2**, again not knowing what material of the coils Demirkhanov used, Copper is perhaps the best material to use to carry current. Not knowing Demirkhanov, it is difficult to give credit to an "illusive" inventor of the Plasma Solenoid, but will give proper credit. The Negative Voltage  $-V$ , **Fig. 3**, on one end of the Copper Coils, and The Positive Voltage  $+V$ , **Fig. 4**, on the other end, creates a current,  $I_s$ , equal to  $(+V - -V)/R = 2V/R$ . The Vacuum, **Fig. 5**, by glass material not shown, is contained in the inside of the Solenoid and the Copper Coils wrapped outside the glass that provide experimentation with Plasmas.

Free-Electron Lasers: A Working Device, *Drawing 2*, use Magnets, **Fig. 6**, and Free Electrons, **Fig. 9**, to cause electrons to bounce back and forth between the Total Reflector, **Fig. 7**, and Output Mirror, **Fig. 8**, creating Light Amplification through Stimulated Emission of Radiation, or LASER. The Magnets, **Fig. 6**, or "wiggler" magnets, cause free-electrons to be produced, and to control the tunability of its frequency. Free Electrons, **Fig. 9**, propagate linearly back and forth from the Total Reflector, **Fig. 7**, to the Output Mirror, **Fig. 8**. The Total Reflector, **Fig. 7**, 100% opaque, causes free-electrons to bounce back in a linear fashion such that most electrons become amplified. The Output Mirror, **Fig. 8**, with a percentage below 100% opaque, causes free-electrons to bounce back and forth until the electrons reach Light Amplification through Stimulated Emission of Radiation causing light to travel outside of the Output Mirror.

Peter Paul Catalasan's Solenoid-Laser System: A Copy of Demirkhanov's Solenoid Experiment with an Addition of Free-Electron Lasers and a Proton Injection Device, *Drawing 3*, uses a Proton Injection



Device, **Fig. 10**, located midway between the Solenoid in order to input pre-plasma protons. Given Demirkhanov's Solenoid, an addition of Two Free-Electron Lasers, **Fig. 11 & Fig. 12**, on the outer ends of the Solenoid, and Electromagnetic Plasma Pinchers at its ends, **Fig. A & Fig. D**, cause plasma confinement radially and in the center of the Solenoid. [As explained earlier,] This Solenoid consists of an Electromagnetic Porous Cylinder Material, **Fig. 15**; Copper Coils, **Fig. 13**, wrapped around the Electromagnetic Porous Cylinder Material, **Fig. 15**; Negative Voltage  $-V$ , **Fig. 17**, and Positive Voltage  $+V$ , **Fig. 16**, in order to cause a current through the Copper Coils, **Fig. 13**, with Plasma confined radially in a Vacuum, **Fig. 14**. Thus the only [two] three additions are the two Free-Electron Lasers, **Fig. 11 & Fig. 12**, [and] a Proton Injection Device, **Fig. 10**, and Electromagnetic Plasma Pinchers, **Fig. A & Fig. D**. Since Free-Electron Lasers work, and the Proton Injection Device very simple, and basic Electromagnetic Plasma Pinchers, and a strait Solenoid, this should work [as well].

The Proton Injection Device, **Fig. 10**, a tiny and almost syringe size injector, inserts, from the Proton Pump (outside), two by two protons,  $2H^+$ , at a time into the Solenoid and Electromagnetic Porous Cylinder where it is received by the Plasma. The Two Free-Electron Lasers, **Fig. 11 & Fig. 12**, on both ends of the Solenoid provide only the clarity of my idea in that the Plasma is linearly centralized near the Proton Injection Device by two opposing lasers. [This will become clear on the next drawing, *Drawing 4*.]

The Electromagnetic Porous Cylinder Material, **Fig. 15**, absorbs the heat generated by the Plasma without contact by having a high-intense electromagnetic field induced by the powerful Solenoid, where its Copper Coils are wrapped around the cylinder material. The Copper Coils, **Fig. 13**, which is wrapped around the Electromagnetic Porous Cylinder Material, **Fig. 15**, must also absorb the heat generated by the Electromagnetic Porous Cylinder Material, and just like the Tokamak Reactor, the Copper Coils must induce an electromagnetic field capable of high-intense pressures to confine the Plasma. The Copper Coils, given Negative Voltage  $-V$ , **Fig. 17**, and Positive Voltage  $+V$ , **Fig. 16**, consist of  $C$  turns and  $L$  layers having power  $P = V^2/R$ , enough to confine Plasma at pressure  $P_p$ . And the Negative Voltage  $-V$ , on one end of the Copper Coils, and The Positive Voltage  $+V$ , on the other end, creates a current,  $I_s$ , equal to  $(+V_s - -V_s)/R = 2V_s/R$ . The Vacuum, **Fig. 14**, not only on the inside, but on the outside as well, creates an environment for the Plasma to be untouched by foreign material. At this point, we just assume that on the outside of the Solenoid, vacuum exists as well, and the details will be provided later on. The two high-intense Electromagnetic Plasma Pinchers, Fig. A & Fig. D, provide linear containment of plasma such that the first, near the center varies its electromagnetic strength, Negative Voltage  $-V_{pv}$ , Fig. B, and Positive Voltage  $+V_{pv}$ , Fig. C, to release the Plasma once it has been used, and the second near the Free-Electron Laser remain fixed in electromagnetic strength, Negative Voltage  $-V_{ps}$ , Fig. E, and Positive Voltage  $+V_{ps}$ , Fig. F, to confine the Plasma, and to allow the passage of the free-electron laser beam into the Solenoid.

Peter Paul Catalasan's Centrifugal-Laser System: A Copy of Demirkhanov's Solenoid Experiment with an Addition of a Free-Electron Laser [and] a Proton Injection Device, and Electromagnetic Plasma Pinchers, in a Centrifuge, *Drawing 4*, uses a Centrifugal Force, **Fig. 18**, equivalent to the Laser Force, **Fig.**

Free-Electron Laser, replacing the other laser by revolving the entire Solenoid at its end on its primary axis. This causes equilibrium between the Force of One Free-Electron Laser, **Fig. 24**, and Centrifugal Force, **Fig. 18**, at the point of the Proton Injection Device, **Fig. 20**. Thus, [again,] Plasma, **Fig. 21**, is confined radially and at its center by the equilibrium forces, in a Vacuum, **Fig. 22**. [Again,] There is an Electromagnetic Porous Cylinder Material, **Fig. 23**, and a Positive Voltage  $+V_s$ , **Fig. 25**, Negative Voltage  $-V_s$ , **Fig. 26**, of the Copper Coils. The One Free-Electron Laser, **Fig. 24**, [have] has Positive Voltage  $+V_L$ , **Fig. 27**, Negative Voltage  $-V_L$ , **Fig. 28**, in order to create Light Amplification through Stimulated Emission of Radiation, or LASER. Since Demirkhanov's Solenoid and One Free-Electron Laser work, the only difference is the Centrifugal Force that replaces on one of its end, a Free-Electron Laser.

The Centrifugal Force, **Fig. 18**, is equivalent to the Laser Force of One Free-Electron as was shown from the previous drawing, *Drawing 3*. Due to the rotation of the Solenoid at its end on its primary axis a Centrifugal Force exists to push the Plasma, **Fig. 21**, at the center of the Solenoid near the Equilibrium Position, where the Proton Injection Device is located, **Fig. 20**. The Centrifugal Force caused by the rotational angular velocity,  $\omega$ , of the Solenoid is on Page 18, called the Theoretical Calculation of the Plasma Centrifugal-Laser Equilibrium Force. The Laser Force, **Fig. 19**, shows the removal of one free-electron laser replaced by the Centrifugal Force. The Force of One Free-Electron Laser, **Fig. 24**, on the other end of the Solenoid, is the Force of One Free-Electron Laser, counteracting the Centrifugal Force imposed on the Plasma, and to center the Plasma at its Equilibrium Position, a location at the Proton Injection Device. The Proton Injection Device, **Fig. 20**, again, a tiny and almost syringe size injector, inserts, from the Proton Pump (outside), two by two protons,  $2H^+$ , at a time bypassing the Solenoid and Electromagnetic Porous Cylinder where the protons are received by the Plasma. The Plasma, **Fig. 21**, having a simple strait solenoid, provides almost unequaled [benefits with] stability and control. The Vacuum, **Fig. 22**, must exist for all Solenoids, the number of which is defined to be  $N_L = (2\pi)/(S+L)*(R-L)$ . At this point, we just assume that on the outside of the Solenoid, and in the inside of the Disk, vacuum exists as well, shown on *Drawing 5*. The Electromagnetic Porous Cylinder Material's, **Fig. 23**, small size, *Drawing 6*, can be misleading since it represents only an ideal solenoid, whereby the actual size can be very large, and thus, did not include constant values [to this application]. Accommodating the Electromagnetic Fields of a powerful Solenoid, the Electromagnetic Porous Cylinder Material must be the same as the material used in the Tomakak Nuclear Fusion Reactor, but in cylindrical form, and also made in the same way. The Negative Voltage  $-V_s$ , **Fig. 26**, on one end of the Copper Coils, and the Positive Voltage  $+V_s$ , **Fig. 25**, on the other end, creates a current,  $I_s$ , equal to  $(+V_s - -V_s)/R_s = 2V/R_s$ . The Copper Coils, consist of C turns and L layers having power  $P_s = V_s^2/R_s$ , in order to confine Plasma at pressure  $P_p$ . The Positive Voltage  $+V_L$ , **Fig. 27**, and the Negative Voltage  $-V_L$ , **Fig. 28**, are the positive and negative voltages connected to the One Free-Electron Laser, attached at the end of the Solenoid. Hence, the Laser Power,  $P_L$ , is  $(+V_L - -V_L) = 2V_L/R_L$ , where the resistance is given by the Laser "Resistance"  $R_L$ . The two Electromagnetic Plasma Pinchers, Fig. G & Fig. J, confine plasma linearly of the strait Solenoid. The first

varies in strength so as to allow used Plasma to exit the Solenoid by pushing the Plasma out with the Free-Electron Laser. The second confines the Plasma on the other end near the Free-Electron Laser that remain fixed and allow passage for the Free-Electron Laser beam.

Rotating Centrifugal-Laser Disk System: A High-Speed Rotating Centrifuged, Proton Injected, and Free-Electron Laser Heated, Electromagnetic Plasma Pinched, Disk System, *Drawing 5*, rotates counterclockwise with Free-Electron Lasers attached at the ends, **Fig. 29**, with Peter Paul Catalasan's Centrifugal-Laser System, **Fig. 30**, and the Proton Injection Device in the Equilibrium Position, **Fig. 31**. Peter Paul Catalasan's Centrifugal-Laser System is tilted in order that the Free-Electron Lasers attached at the ends do not shoot each other, **Fig. 32**. The tilt at the Center Hole, **Fig. 33**, shows Free-Electron Laser paths that push the Plasma, when it is no longer useful for energy, into the Center Hole and into the Plasma Exhaust System. The Energy released is absorbed by the Electromagnetic Porous Cylinder Material transferring heat energy to the Heat Sink, **Fig. 34**, and into the surrounding water medium. The entire Disk System, on the outside skin, is covered with Near Frictionless Carbon Coating developed by Argonne National Laboratory, with the coefficient of friction less than 0.001 [4].

The Free-Electron Lasers attached at the ends, **Fig. 29**, are in a circular pattern, D length, L width, and S circumference apart, with the number of lasers,  $N_L = (2\pi)/(S+L)*(R-L)$ , where R is the Radius. The highly tunable free-electron laser, attached at the ends, provide the Equilibrium Force needed to maintain the Plasma at the Equilibrium Position, **Fig. 31**. The Peter Paul Catalasan's Centrifugal-Laser System, **Fig. 30**, shows the Solenoid described from the previous drawing, *Drawing 4*. The Proton Injection Device in the Equilibrium Position, **Fig. 31**, located midway between the Solenoids, injects, two by two protons,  $2H^+$ , into the Plasma, described from the previous drawing, *Drawing 4*. The Free-Electron Lasers attached at the ends do not shoot each other, **Fig. 32**, shows Free-Electron Laser paths, tilted in order to keep the lasers from shooting each other. The laser paths contain tiny small holes drilled within the Heat Sink, **Fig. 34**, and at its end, a Laser Absorption Device that recovers the energy of the Free-Electron Laser, which transfers the laser heat energy into the Heat Sink, **Fig. 34**. The Center Hole, **Fig. 33**, 2A in diameter, provides the exit of used Plasma by Free-Electron Lasers pushing the Plasma into a hole where a current carrying electromagnetic plate, then, pushes it to the Plasma Exhaust System, **Fig. 43**, after the Variable Electromagnetic Plasma Pincher, Fig. M, lowers its strength to allow the passage of Plasma. The Heat Sink, **Fig. 34**, a Titanium Alloy, encase all the Solenoids and Free-Electron Lasers in order to absorb the heat generated by the Plasma, releasing the energy to the surrounding water medium.

Peter Paul Catalasan's Centrifugal-Laser System: A Copy of Demirkhanov's Solenoid Experiment with an Addition of a Free-Electron Laser and a Proton Injection Device in a Centrifuge, *Drawing 6*, consist of a Proton Injection Device, Electrical Wire System, Demirkhanov's Solenoid, Free-Electron Laser, Electromagnetic Plasma Pinchers, and Plasma Exhaust System. The Proton Injection Device consists of the Proton Pump from the outside, **Fig. 34**, Proton Capture, **Fig. 35**, and Proton Rotating Mechanical Seal, **Fig. 36**, where the Proton is pushed down into the Proton Injection Device that contains a small Electrical

Switch, Fig. 40, toggling between positive and negative charge in order to trap protons and push them into Demirkhanov's Solenoid. The Electrical Wire System consists of Wire Inputs, Fig. 37, Rotating Wire Contacts, Fig. 38, Electrical Wires, Fig. 39, and a Wire Rotating Mechanical Seal. The Electrical Wires contain wires from the Free-Electron Laser,  $+V_L$  &  $-V_L$ , Demirkhanov's Solenoid,  $+V_S$  &  $-V_S$ , Plasma Exhaust Solenoid,  $+V_E$  &  $-V_E$ , and Electromagnetic Plate, Fig. 41,  $+V_P$  &  $-V_P$ . The Plasma Exhaust System consists of an Electromagnetic Plate, Fig. 41 & Fig. 42, an Exhaust Solenoid, Fig. 44, with Copper Coils, Fig. 43. Finally, Titanium Alloy, Fig. 45, encloses all the Proton Injection Device, Demirkhanov's Solenoid and Free-Electron Laser, Electrical Wire System, Electromagnetic Plasma Pinchers, and Plasma Exhaust System.

The Proton Injection Device consists of the Proton Pump, Fig. 34, from the outside of the Water Reactor, the Proton Capture, Fig. 35, the Rotating Mechanical Seal, Fig. 36, and the Electrical Switch, Fig. 40. The Proton Pump from the outside, Fig. 34, pumps Protons,  $H^+$ , into the Proton Capture, Fig. 45, through a Proton Rotating Mechanical Seal, Fig. 36. Centrifugal and rotary positive displacement pumps require controlling of the pumped Hydrogen's desire to exit through the stuffing box, the area where the pump shaft enters the pump Hydrogen's end. When operating, the pumped Hydrogen within the stuffing box sees a pressure higher than the surrounding atmospheric pressure, and on static lift applications; during the priming cycle, the stuffing box will see a pressure below atmospheric pressure i.e., a vacuum. In either operating condition a mechanical seal will virtually eliminate the release of the pumpage to atmosphere and the entrance of air into a stuffing box when under vacuum. The Proton Capture, Fig. 35, captures protons that are pumped from the outside, in such a way as to rotate with two thin flat disks and small shaft that leads to the Electrical Switch, Fig. 40. The material is Titanium Alloy. The Proton Rotating Mechanical Seal, Fig. 36, is not a complex device. It consists primarily of a rotary seal face with a driving mechanism which rotates at the same speed as the pump shaft, a stationary seal face which mates with the rotary and is retained using a gland or in some pump models an integral stuffing box cover, a tension assembly which keeps the rotary face firmly positioned against the stationary face to avoid leakage when the pump is not in operation, and static sealing gaskets and elastomers strategically located to complete the assembly [4].

The Electrical Switch, Fig. 40 is a switch that toggles between positive and negative charge. When positive, the switch closes the paths of protons since a positive charge and a positive proton repels. And, when the switch is negative, it attracts protons since a negative charge and a positive proton is opposite in charge. Now, when the switch turns positive again, it repels the protons and pushes it down the tiny syringe size injector, and into the Plasma. The Electrical Wire System, consist of the Wire Inputs, Fig. 37, Rotating Wire Contacts, Fig. 38, Electrical Wires, Fig. 39, Wire Rotating Mechanical Seal, Free-Electron Laser,  $+V_L$  &  $-V_L$ , Demirkhanov's Solenoid,  $+V_S$  &  $-V_S$ , Variable Electromagnetic Plasma Pincher,  $+V_{pv}$  &  $-V_{pv}$ , and Fixed Electromagnetic Plasma Pincher,  $+V_{ps}$  &  $-V_{ps}$ , Plasma Exhaust Solenoid,  $+V_E$  &  $-V_E$ , and Electromagnetic Plate,  $+V_P$  &  $-V_P$ , Fig. 41, all encased with Titanium Alloy, Fig. 45. The Wire Inputs, Fig. 37, come from the outside of the Water Reactor, *Drawing 8*, Fig. 57. The wire inputs lead directly to

the Rotating Wire Contacts, **Fig. 38**. The Rotating Wire Contacts, **Fig. 38**, contain wires that connect to corresponding rings that maintain contact with the outside wires while the rings rotate counterclockwise. The Electrical Wires, **Fig. 39**, consist of the wires for the Electrical Toggle Switch, Free-Electron Laser,  $+V_L$  &  $-V_L$ , Demirkhanov's Solenoid,  $+V_S$  &  $-V_S$ , Variable Electromagnetic Plasma Pincher,  $+V_{pv}$  &  $-V_{pv}$ , and Fixed Electromagnetic Plasma Pincher,  $+V_{ps}$  &  $-V_{ps}$ , Plasma Exhaust Solenoid,  $+V_E$  &  $-V_E$ , and Electromagnetic Plate,  $+V_P$  &  $-V_P$ . The Wire Rotating Mechanical Seal, consists primarily of a rotary seal face with a driving mechanism which rotates at the same speed as the pump shaft, a stationary seal face which mates with the rotary and is retained using a gland or in some pump models an integral stuffing box cover, a tension assembly which keeps the rotary face firmly positioned against the stationary face to avoid leakage when the pump is not in operation, and static sealing gaskets and elastomers strategically located to complete the assembly [4].

The Free-Electron Laser,  $+V_L$  &  $-V_L$ , is the same laser device mentioned above with its wires leading to the Rotating Wire Contacts. The Demirkhanov's Solenoid,  $+V_S$  &  $-V_S$ , also, is a solenoid device with properties mentioned before and its wires leading to the Rotating Wire Contacts. The Variable Electromagnetic Plasma Pincher,  $+V_{pv}$  &  $-V_{pv}$ , **Fig. P & Fig. Q**, and Fixed Electromagnetic Plasma Pincher,  $+V_{ps}$  &  $-V_{ps}$ , **Fig. S & Fig. T**, control the strengths of the electromagnetic fields produced, with wires that lead to the Rotating Wire Contacts, **Fig. 38**. The Plasma Exhaust Solenoid,  $+V_E$  &  $-V_E$ , **Fig. 44**, is a hyperbolic solenoid cylinder that receives used Plasma from Demirkhanov's Solenoid and the Electromagnetic Plate, **Fig. 41**, pushes it to the Plasma Exhaust System, *Drawing 7*. The Electromagnetic Plate,  $+V_P$  &  $-V_P$ , **Fig. 41**, is a current-carrying electromagnetic plate located above the Center Hole, **Fig. 42**, causing Plasma to be pushed into the Plasma Exhaust System, *Drawing 7*. The Plate's wires are also connected to the Rotating Wire Contacts, **Fig. 38**. The Titanium Alloy, **Fig. 45**, encases all the components of this entire Catalasan Centrifugal-Laser Nuclear Fusion Reactor, *Drawing 6*, *Drawing 7*, and *Drawing 8*.

The Plasma Exhaust System: Exploded View, *Drawing 7*, consist of the Titanium Alloy, **Fig. 46**, Rotating Mechanical Seal, **Fig. 47 & Fig. 48**, Exhaust Solenoids, Two Free-Electron Lasers from the outside, Plasma Exit Solenoids, and Electrical Wire System, **Fig. 49**, contain Exhaust Solenoid Voltages,  $-V_E$  &  $+V_E$ , all rotating counterclockwise. The Titanium Alloy, **Fig. 46**, revolving counterclockwise, encase the hyperbolic solenoids using a Rotating Mechanical Seal, **Fig. 47 & Fig. 48**.

The Rotating Mechanical Seal, **Fig. 47 & Fig. 48**, is fixed in space with two Free-Electron Lasers and two Plasma Exit Solenoids, where the hyperbolic solenoids and Titanium Alloy casing rotate counterclockwise. The Rotating Mechanical Seal is similar to the Proton Mechanical Seal. Thus, it consists primarily of a rotary seal face with a driving mechanism which rotates at the same speed as the pump shaft, a stationary seal face which mates with the rotary and is retained using a gland or in some pump models an integral stuffing box cover, a tension assembly which keeps the rotary face firmly positioned against the stationary face to avoid leakage when the pump is not in operation, and static sealing gaskets and elastomers strategically located to complete the assembly [4]. The Exhaust Solenoids, consist

of the top and bottom hyperbolic solenoids joined and rotating, but the Rotating Mechanical Seal fixed in space. The Two Free-Electron Lasers from the outside push the used Plasma outside of the Disk System. The Plasma Exit Solenoids are pipe-like solenoids that transfer the used Plasma pushed by Free-Electron Lasers outside of the Water Reactor. The Electrical Wire System, **Fig. 49**, provides power to the Solenoids such that its wires connect to the Electrical Wires, *Drawing 6*, **Fig. 39**. The Exhaust Solenoid Voltages,  $-V_E$  &  $+V_E$ , creates a current,  $I_E$ , equal to  $(+V_E - -V_E)/R_E = 2V/R_E$ . The Copper Coils of the Exhaust Solenoids, given Negative Voltage  $-V_E$ , and Positive Voltage  $+V_E$ , consist of  $C_E$  turns and  $L_E$  layers having power  $P_E = V_E^2/R_E$ , to confine Plasma at pressure  $P_E$ .

The last drawing, the Catalasan Centrifugal-Laser Nuclear Fusion Reactor: A High-Speed Rotating Centrifugal-Laser & Steam-Turbine Nuclear Fusion Reactor, designated as the Main Drawing, *Drawing 8*, is the integration of a Flip-Flopped Rotating Centrifugal-Laser Disk System, **Fig. 58**, Plasma Exhaust System, **Fig. 57**, Steam Turbine System, **Fig. 50**, and Electric Turbine Generator, **Fig. 61**. The Flip-Flopped Rotating Centrifugal-Laser Disk System, **Fig. 58**, consists of the Rotating Centrifugal-Laser Disk System [on], *Drawing 5*, stacked such that the Plasma Exhaust System is joined together and the Proton Pump, Proton Injection System, and Electrical Wire System [on], *Drawing 6*, are also joined together, **Fig. 57**, all rotating through the Steam-Turbine Gear System, **Fig. 52**, due to Steam, **Fig. 51**, passing through Steam Turbines, **Fig. 50**. The Steam, then, is condensed through a Steam Condenser, **Fig. 54**, through Steam Pipes, **Fig. 53**, and into the  $H_2O$  Reservoir, **Fig. 55**, which is then connected by an Open Valve, **Fig. 56**, back into the Reactor. The Rotation caused by the Steam-Turbine Gear, **Fig. 52**, is then translated, by the Axle, **Fig. 60**, to the Electric Power Turbine Generator, **Fig. 61**, generating Commercial Electricity, **Fig. 62**, with a gear connected Gas Turbine Engine Starter, **Fig. 59**.

The Flip-Flopped Rotating Centrifugal-Laser Disks, **Fig. 58**, are Rotating Centrifugal-Laser Disk Systems, *Drawing 5*, flip-flopped such that the Proton Capture, Electrical Wire System are joined together, and the Plasma Exhaust System are also joined together; in other words, upside down and right side up. The Plasma Exhaust System, **Fig. 57**, contains two Free-Electron Lasers from the outside of the Water Reactor that push used Plasma outside on the other side by a pipe-like Solenoid. The Steam Turbine System, **Fig. 50**, consists of four Steam Turbines, with power  $4P$  found by the Theoretical Calculation of the Power Generated by One of Four Steam Turbines, *Page 16*, such that each rotating steam turbine gear is attached to the center axle disk, **Fig. 51**. The Electric Turbine Generator, **Fig. 61**, is an electric turbine generator of electricity available in the market. The Steam-Turbine Gear System, **Fig. 52**, uses a spiral bevel gear such that the ratio is one to four between the spiral bevel gear and the gear of one of four steam turbines. The Steam, **Fig. 51**, is a superheated water vapor that enters into each of the four steam turbines. The Steam Pipes, **Fig. 53**, transfers the superheated water vapor to the condenser, available in the market. The Steam Condenser, **Fig. 54**, allows the superheated water vapor to condense into a saturated water vapor mixture that enters the  $H_2O$  Reservoir by steam pipes. The  $H_2O$  Reservoir, **Fig. 55**, consist of water in a container that acts as a buffer in transferring the water from the Condenser to the Water Reactor through an

Open Valve. The Open Valve, **Fig. 56**, transfers H<sub>2</sub>O back to the Main Water Reactor using a pipe with a variable open valve. The Axel, **Fig. 60**, is the primary axis at which this entire system rotates with angular velocity  $\omega$ . The Commercial Electricity, **Fig. 62**, provides electricity to the commercial public. The Gas Turbine Engine Starter, **Fig. 59**, starts the system by rotating the Axel, **Fig. 60**, counterclockwise until the system approaches the working angular velocity  $\omega$ , after which the gear connection to the Axel from the Gas Turbine Engine Starter, detaches using a [simple] gear system. [similar to automobiles.]

How to Start the Reactor, *Drawing 8*, begins with the Gas Turbine Engine Starter, **Fig. 59**, which rotates the Axel, **Fig. 60**, at the angular velocity  $\omega$ , with the Theoretical Calculation of the Mechanical Speed Limit with or without Temperature of the Centrifugal-Laser Spinning Disk System, *Page 17*. All the Solenoids must start, before rotation, their electromagnetic fields through the Electrical Wire System, *Drawing 6*, **Fig. 39**. After determining the angular velocity  $\omega$ , we find the Theoretical Calculation of the Plasma Centrifugal-Laser Equilibrium Force, *Page 18*, or the Laser Force, which will trap the Plasma linearly. The Proton Injection Device, *Drawing 6*, **Fig. 40**, then inserts protons two by two until there are  $4p \cdot N_p$ , the multiple number of four protons times  $N_p$ . After the Plasma is pinched by high-intense Electromagnetic Plasma Pinchers, the Free-Electron Lasers begin heating the protons to the temperature of  $4 \times 10^8$  Kelvin, in which the Plasma begins to release Nuclear Energy transferring the heat to the Rotating Centrifugal-Laser Disk System, *Drawing 5*, where the heat sink, Titanium Alloy Disk, in turn releases the heat to the Water Reactor causing a temperature increase  $T$ . Given the Temperature  $T$ , we determine the Pressure  $P$  of the Water Reactor through the Theoretical Calculation of the Water Reactor Pressure and Volume given Temperature  $T$ , *Page 14*. The increase in Pressure then turns the Steam Turbine System, causing automatic rotation of the Axel and in turn the Electric Turbine Generator, *Drawing 8*, **Fig. 61**. Once everything is stable, through the Steam Turbine System rotating at a constant angular velocity  $\omega$ , the Gas Turbine Starter detaches its gear.

Since the components of this system work and exist in the market today, it implies that this Nuclear Fusion Reactor will also work, where Demirkhanov's Solenoid [is] as a viable proof of experimentation, and this application is mostly its integration. This Fusion Reactor can have multiple Disks, stacked flip-flopped on top of each other for more fusion power when appropriately needed. And, for uses in Space, one requires a counter rotation mechanism not mentioned in this patent application.

The practical design of this fusion engine is its simplicity, ease of use, maintenance, and safety far better than any Nuclear [Fission] Reactor[s]. [free from harmful radiation. And, the simplicity of this Reactor makes maintenance far better than any Nuclear Fusion Reactor Design.] Using high-pressure water and steam, it also has a direct rotating Axel for mechanical applications. Considering the military uses of this Reactor, it can never be used for weapons of mass destruction. [Moreover, using high-pressure water and steam makes this *Catalasan Nuclear Fusion Reactor* so environmentally friendly that I believe this design merits praise from myself as well.]

## VI. Theoretical Calculations

### Theoretical Calculation of the Water Reactor Pressure and Volume given Temperature T

■ **Problem Statement:** Given Temperature T, High Pressure and Volume exists due to a superheated water vapor mixture of the Water Reactor. Find the Pressure P and Volume V.

Equivalent Mathematical Model of the Problem Statement: [10]

A rigid tank contains  $m_t$  kg of water at temperature. If  $m_g$  kg of the water is in the liquid form and the rest is in the vapor form, determine the (a) pressure P in the tank and (b) volume V of the tank.

A rigid tank contains saturated mixture. The pressure and the volume of the tank are to be determined.

(a) Since the two phases coexist in equilibrium, we have a saturated superheated water vapor mixture and the pressure must be the pressure at the given temperature:

$$P = P_T = \text{from (Table A-6) at temperature } T$$

(b) We must determine the quality  $x$ , then the average specific volume  $v$ , and finally find the total volume V:

$$x = \frac{m_g}{m_t}$$

$$v = v_f + x v_{fg} \quad \text{and}$$

$$V = nv \quad \text{where } m \text{ is the total mass.}$$



## Theoretical Calculation of the Cylinder Thickness of the Water Reactor

- **Problem Statement:** Given the increase in heat and temperature by Centrifugal-Laser Rotating Disks, Pressure P builds upon the walls of the Water Reactor. Find the thickness necessary to contain the water pressure.

Equivalent Mathematical Model of the Problem Statement: [1]

A cylinder with end caps is to have inner radius  $b$ . It must carry internal pressure  $P$  with safety factor  $SF = 1.7$ . Failure is defined as the onset of yielding. The material yields at uniaxial tensile stress  $\sigma_Y$ . According to the maximum shear stress failure criterion, what must be outer radius  $a$ ? Under the working pressure of  $P$ , what is the radial expansion at  $r = b$  and at  $r = a$ ? Use  $E = 204 \text{ GPa}$  and  $\nu = 0.29$

Radius  $a$  can be determined from  $r = b$ :

$$\tau_{\max} = \frac{pa^2}{a^2 - b^2} \quad \text{where} \quad p = p_i \text{ or } p = p_o$$

using  $\tau_{\max} = \sigma_Y / 2$ , and design pressure  $p_i = (SF) 140$ ; We obtain the variable  $a$ .

At the working pressure  $p_i$  we get  $\sigma_r, \sigma_\theta, \sigma_z$ , from the same equation.

Circumferential strain is  $\epsilon_\theta = [\sigma_\theta - \nu(\sigma_z + \sigma_r)] / E$ . Evaluating this at  $r = b$ , we obtain  $\epsilon_{\theta b}$  using this same equation. Also, since

$$\epsilon_\theta = \frac{u}{r} \quad \text{we get } u_b = b \epsilon_{\theta b} \quad \text{and}$$
$$u_a = a \epsilon_{\theta a} \quad \text{for } r = a.$$

Used with permission of Pearson Education, Inc., Upper Saddle River, NJ.

## Theoretical Calculation of the Power Generated by One of Four Steam Turbines

- **Problem Statement:** Steam in a superheated vapor state enters and exits one adiabatic Steam Turbine with the power output,  $P$ . Determine the Work done per unit mass of Steam flowing through the Turbine. And, Calculate the mass flow rate of the Steam.

Equivalent Mathematical Model of the Problem Statement: [10]

The power output of an adiabatic Steam Turbine is  $P$  MW (MegaWatts), and the inlet and the exit conditions of the Steam are as follows:

In: $P_1$ , pressure = $P/4$ turbines	Out: $P_2$ , pressure
$T_1$ , temperature	$x_2$ , temperature
$V_1$ , velocity	$V_2$ , velocity
$z_1$ , potential energy height	$z_2$ , potential energy height

a) Determine the work done per unit mass of the Steam flowing through the turbine.

b) Calculate the mass flow rate of the Steam

We take the *Turbine* as the system. This is a control volume since mass crosses the system boundary during the process. We observe that there is only one inlet and one exit and thus  $\dot{m}_1 = \dot{m}_2 = \dot{m}$ . Also, work is done by the system. The inlet and exit velocities and elevations are given, and thus the kinetic and potential energies are to be considered. This is a steady-flow process since there is no change with time at any point. The system is adiabatic and thus there is no heat transfer.

Given  $P_1$  and  $T_1$  and Steam in a superheated vapor state, we can find the enthalpy  $h_1$  from a table of pressures and temperature. At the turbine exit, we have a saturated liquid-vapor mixture therefore the enthalpy is  $h_2 = h_f + x_2 h_{fg}$ . Then, the change in enthalpy is,  $\Delta h = h_2 - h_1$ . The change in kinetic energy is  $\Delta ke = (V_2^2 - V_1^2)/2$ . The change in potential energy is  $\Delta pe = g(z_2 - z_1)$ .

The energy balance for this steady-flow system can be expressed in the rate form as follows:

The rate of net energy transfer by heat, work, and mass =  $E_{in} - E_{out} = \Delta E_{system} = 0$  = rate of change in internal, kinetic, potential, etc., energies  $E_{in} = E_{out}$ . Thus, work done is:

$$\dot{m} (h_1 + V_1^2/2 + g z_1) = \dot{W}_{out} + \dot{m} (h_2 + V_2^2/2 + g z_2) \text{ Since } \dot{Q} = 0$$

Dividing by the mass flow rate  $\dot{m}$  and substituting, the work done by the turbine per unit mass of the Steam is determined to be  $w_{out} = -(\Delta h + \Delta ke + \Delta pe)$  and the required mass flow rate for a  $P$  MW (MegaWatts) is

$$\dot{m} = \frac{\dot{W}_{out}}{w_{out}}$$

## Theoretical Calculation of the Mechanical Speed Limit with or without Temperature of the Centrifugal-Laser Spinning Disk System

- **Problem Statement:** There is a Mechanical Failure Limit of a rotating Centrifugal-Laser Disk System with a hole at its center and Lasers attached at the ends, such that, it is all encased by Titanium Alloy. Find the Stresses and the Speed that will cause failure. Also, find the failure due to Temperature T.

Equivalent Mathematical Model of the Problem Statement: (Stresses & Speed) [1]

A Metal Disk,  $t$  thick and  $2a$  in diameter, is attached to a solid metal shaft,  $2s$  in diameter, by means of shrink-fit (equal strength). The hole in the Disk is  $2b$  in diameter before it is attached to the shaft. What is the largest normal stress at standstill? At what speed will the shrink-fit loosen, and what are the stresses at this speed? Let  $E$  be the pressure,  $\rho$  be the density, and  $v$ , the velocity.

For shrink-fit analysis at standstill, we will assume that the shaft can be treated as a solid disk of the same thickness as the annular disk. Due to contact pressure  $p_c$ , stresses in the shaft are  $\sigma_r = -p_c$  and  $\sigma_\theta = -p_c$ . And, stresses at  $r = b$  in the annular disk are  $\sigma_r = -p_c$  and  $\sigma_\theta = 1.093 p_c$ . Circumferential strains must create a radial gap of 0.0001 meters at  $r = 0.08$  meters. Hence, applying the radial displacement equation  $u = r(\sigma_\theta - \nu \sigma_r)/E$  to each part, we write

$$0.0001 = \frac{0.08}{E} (1.093 p_c - \nu (-p_c)) - \frac{0.08}{E} (-p_c - \nu (-p_c))$$

from which we find  $p_c$ . The largest normal stress at standstill is therefore  $\sigma_\theta$ , given  $r$  in the annular disk.

Until the shrink-fit loosens, stresses due to spinning can be calculated as if the disk-plus-shaft assembly were a single solid disk. These stresses are superposed on stresses caused by  $p_c$ . The loosening speed  $\omega_L$  is defined as the speed at which net radial stress at  $r = 0.08$  meters becomes zero. Thus, for a flat solid disk,

$$0 = \frac{3+\nu}{8} \rho \omega^2 a^2 \left(1 - \frac{r^2}{a^2}\right) \text{ and } \omega, \text{ the maximum angular speed follows}$$

Equivalent Mathematical Model of the Problem Statement: (Temperature)

A solid disk and an annular disk, of the same thickness but different materials, fit together exactly. What state of stress is produced by uniformly increasing the temperature of the annular disk an amount  $T$ ?

A compatibility condition occurs, at  $r = c$ :  $(u \text{ due to } p_c, \text{ and } T)_{\text{outer}} = (u \text{ due to } p_c)_{\text{inner}}$

Stresses in the solid disk are  $\sigma_r = -p_c$  and  $\sigma_\theta = -p_c$  throughout. Therefore the compatibility equation becomes:

$$\frac{c}{E_o} [p_c \frac{a^2 + c^2}{a^2 - c^2} - \nu_o (-p_c)] - c \alpha_o T = \frac{c}{E_i} [-p_c - \nu_i (-p_c)]$$

Same material: 
$$p_c = \frac{E \alpha T (a^2 - c^2)}{2 a^2}$$

Stresses in the annular disk: For  $r > c$ : 
$$\sigma_r = \frac{E \alpha T}{2} \left( \frac{c^2}{a^2} - \frac{c^2}{r^2} \right), \quad \sigma_\theta = \frac{E \alpha T}{2} \left( \frac{c^2}{a^2} + \frac{c^2}{r^2} \right),$$

from which  $T$  follows

Used with permission of Pearson Education, Inc., Upper Saddle River, NJ.

## Theoretical Calculation of the Plasma Centrifugal-Laser Equilibrium Force

- **Problem Statement:** Plasma moves linearly along the primary axis of a strait solenoid revolved at its end and primary axis in a disk centrifuge, with an equivalent opposite laser force that causes plasma to stay in equilibrium position. Find the Force.

Equivalent Mathematical Model of the Problem Statement: [1]

A bead (plasma center of mass) moves along the spoke of a wheel at constant speed  $u$  meters per second. The wheel rotates with uniform angular velocity  $\theta = \omega$  radians per second about an axis fixed in space. At  $t = 0$  the spoke is along the  $x$ -axis, and the bead (plasma center of mass) is at the origin. Using Cartesian Coordinates, find the velocity at time  $t$ . Then, find the Centrifugal Force at time  $t$ .

$$V_x = V_r \cos \theta - V_\theta \sin \theta \quad V_y = V_r \sin \theta + V_\theta \cos \theta$$

Since,  $V_r = u$ ,  $V_\theta = r\omega = u\omega$ ,  $\theta = \omega t$ , we obtain

$$\vec{V} = u(\cos \omega t - \omega t \sin \omega t) \hat{i} + u(\sin \omega t + \omega t \cos \omega t) \hat{j}$$

In[6]:=

$$X = \text{Integrate}[u(\cos[\omega t] - \omega t \sin[\omega t]), u, t]$$

$$\text{Out[6]} = \frac{1}{2} t u^2 (\cos[\omega t] - \omega t \sin[\omega t])$$

In[7]:=

$$Y = \text{Integrate}[u(\sin[\omega t] + \omega t \cos[\omega t]), u, t]$$

$$\text{Out[7]} = \frac{1}{2} t u^2 (\sin[\omega t] + \omega t \cos[\omega t])$$

$$\vec{a} = \frac{1}{2} t u^2 (\cos[\omega t] - \omega t \sin[\omega t]) \hat{i} + \frac{1}{2} t u^2 (\sin[\omega t] + \omega t \cos[\omega t]) \hat{j}$$

Where  $u = \frac{r}{t}$ , and  $\vec{F} = m\vec{a}$  Therefore, the Centrifugal Equilibrium Force is

$$\vec{F} = \frac{1}{2} m t u^2 (\cos[\omega t] - \omega t \sin[\omega t]) \hat{i} + \frac{1}{2} m t u^2 (\sin[\omega t] + \omega t \cos[\omega t]) \hat{j}$$

Used with permission of Pearson Education, Inc., Upper Saddle River, N.J.

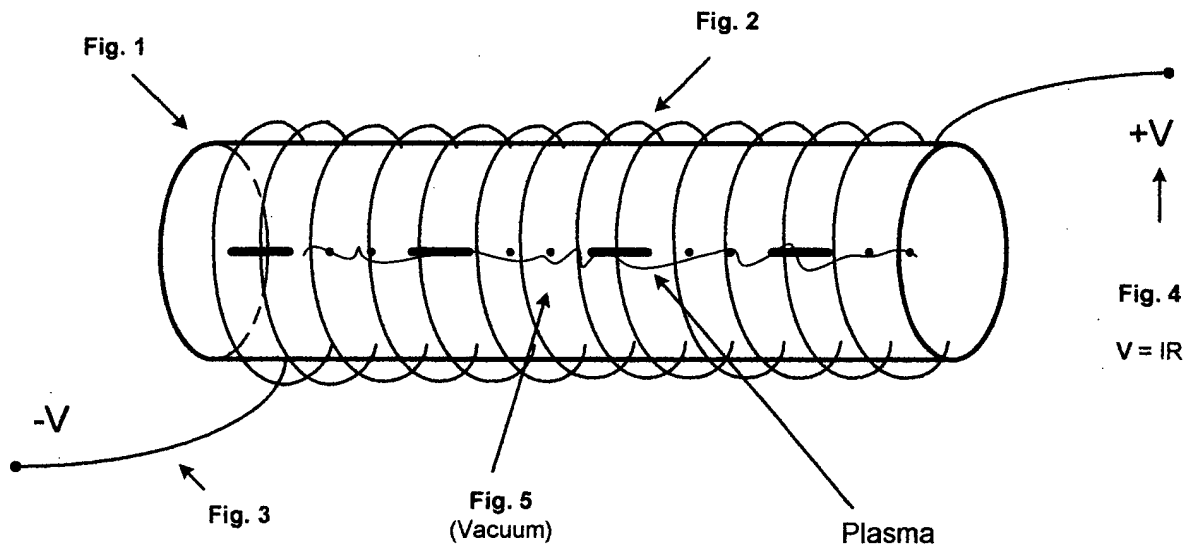
VII. [Reference] Bibliography

- [1] Advanced Mechanics of Materials 2/E, Cook R & Young W © 1999
- [2] An Introduction to Mechanics, Kleppner & Kolenkow
- [3] Electromagnetic Fields 2<sup>nd</sup> Edition, Wangsness
- [4] Internet and the World Wide Web
- [5] Introduction to Plasma Physics and Controlled Fusion 2<sup>nd</sup> Edition, Chen
- [6] Lasers, Siegman
- [7] Mathematica Software v4.2 for Students, Stephen Wolfram
- [8] Mathematical Methods for Physicists 5<sup>th</sup> Edition, Arfken & Weber
- [9] The Physics of Laser-Atom Interactions, Suter
- [10] Thermodynamics: An Engineering Approach 4<sup>th</sup> Edition, Cengel & Boles

# Demirkhanov's Solenoid Experiment

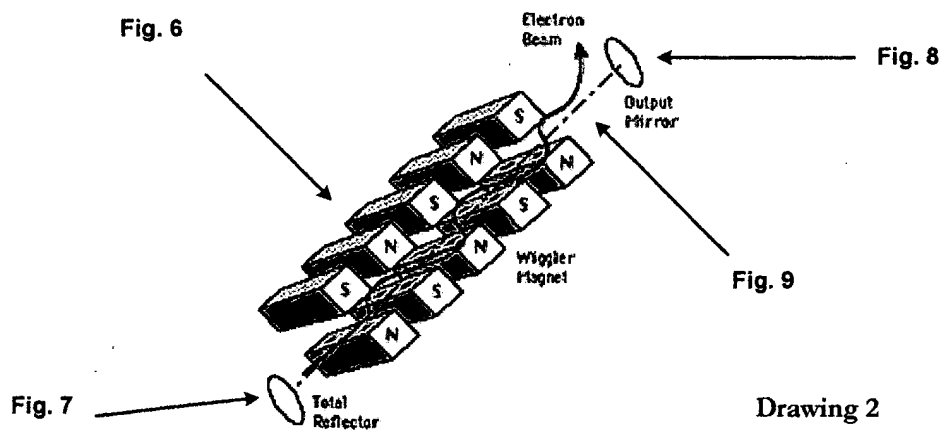
## *A Working System*

Drawing 1



# Free-Electron Lasers

## *A Working Device*



Drawing 2

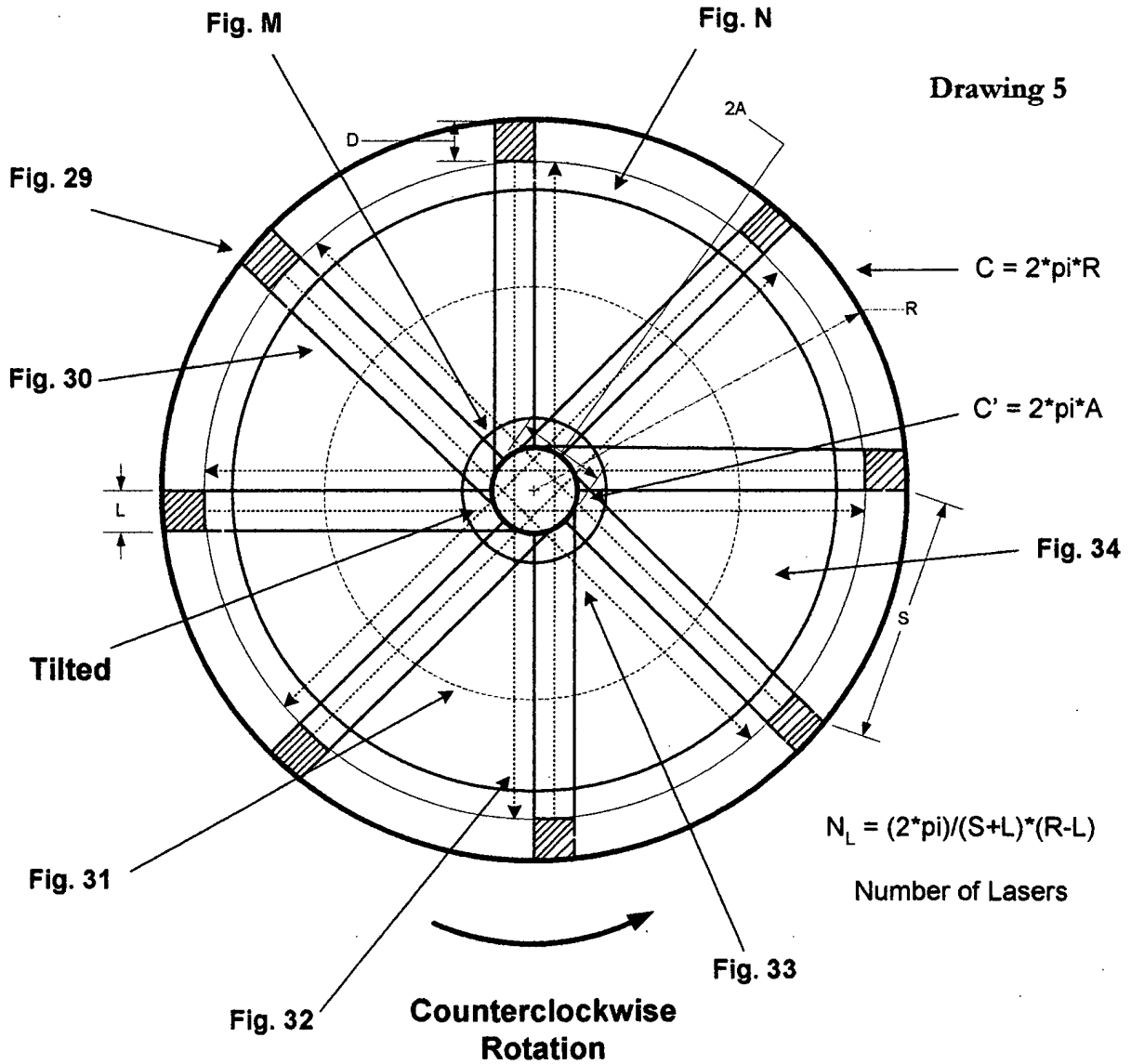






# Rotating Centrifugal-Laser Disk System

*A High-Speed Rotating Centrifuged, Proton Injected,  
and Free-Electron Laser Heated, Disk System*



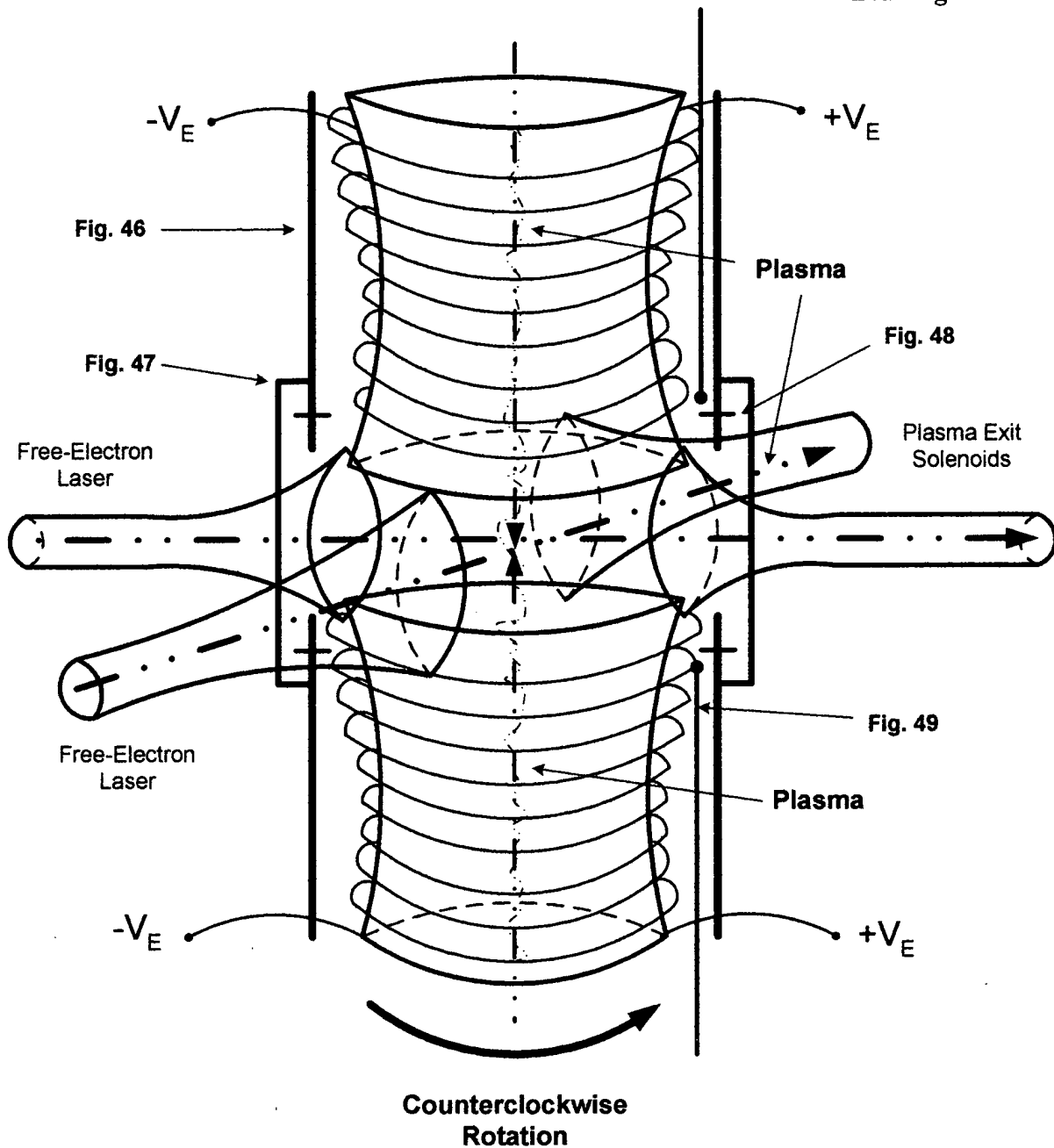
*A Copy of Demirkanov's Solenoid Experiment with an Addition of a Free-Electron Laser and a Proton Injection Device in a Centrifuge*



# Plasma Exhaust System

*Exploded View*

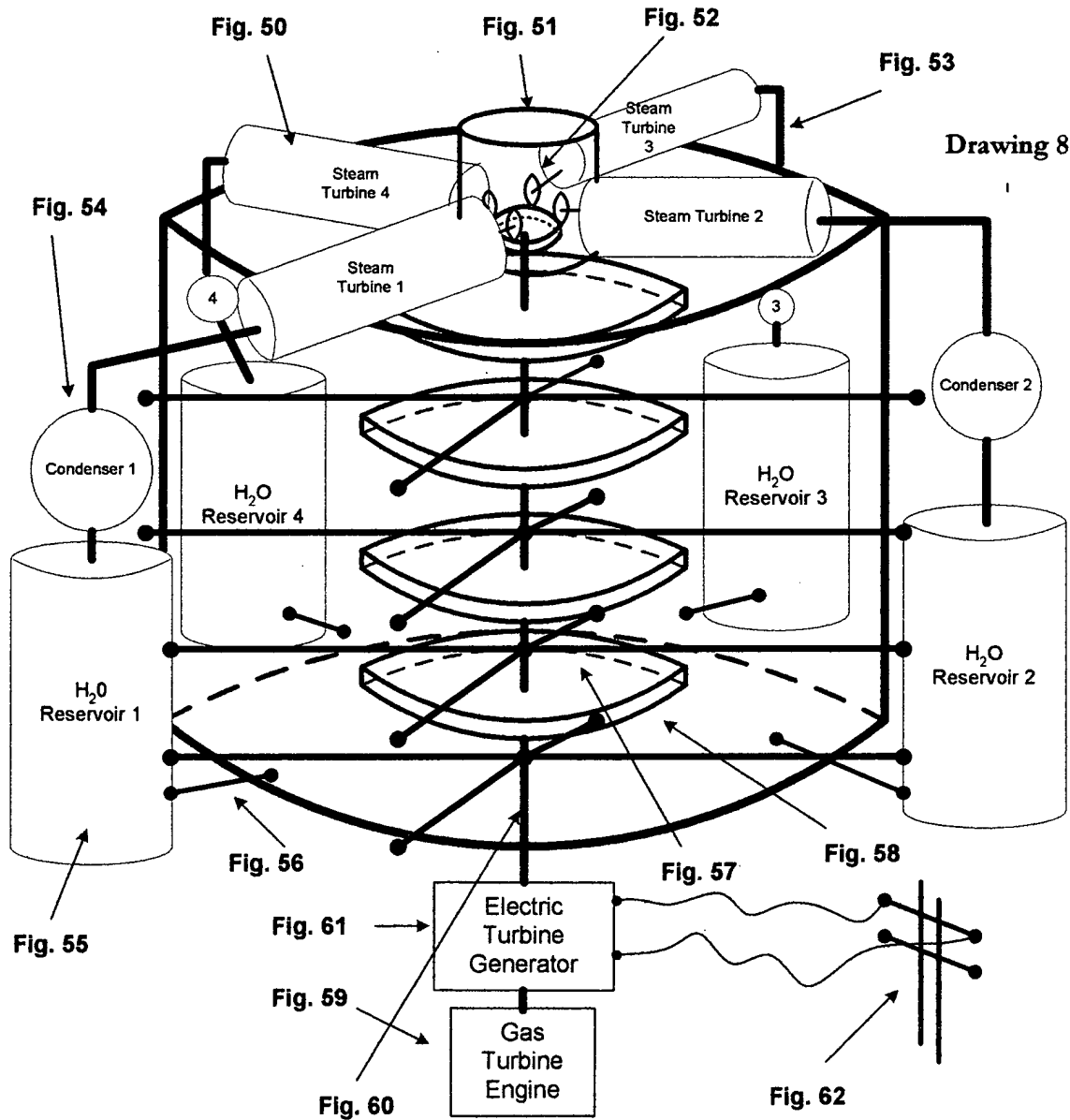
Drawing 7



# Catalasan Centrifugal-Laser Nuclear Fusion Reactor

A High-Speed Rotating Centrifugal-Laser & Steam-Turbine Nuclear Fusion Reactor

[Designated as the Main Drawing]



**“CATALASAN NUCLEAR FUSION REACTOR”**  
**A High Speed Rotating Centrifugal-Laser**  
**Nuclear Fusion Reactor**

**Mr. Peter Paul Catalasan**

Chief Theoretical Research Scientist:

A Mathematical Physicist,

Theoretical Computer Scientist, and

Artificial Intelligence Researcher

Advanced Catalasan Research Laboratories, Inc.

Citizen of the Republic of the Philippines

Citizen of the United States of America

*CSULB Graduate Student*

United States Residence

25410 Dodge Ave. # K

Harbor City, CA 90710

[pcatalas@engr.csulb.edu](mailto:pcatalas@engr.csulb.edu)

310.830.1046

**Catalasan Nuclear Fusion Reactor Claims:**

1. Thermonuclear Fusion Reactor
2. Electrical Energy Generation Plant
3. Submarine Power Plant
4. Spacecraft Power Plant
5. Scalable Power Plant